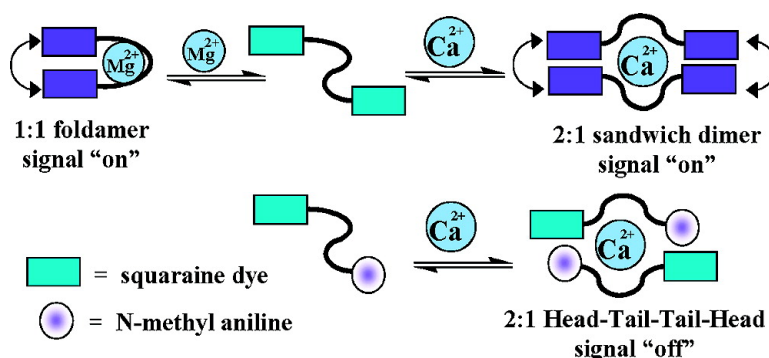


A Controlled Supramolecular Approach toward Cation-Specific Chemosensors: Alkaline Earth Metal Ion-Driven Exciton Signaling in Squaraine Tethered Podands

Easwaran Arunkumar, Parayali Chithra, and Ayyappanpillai Ajayaghosh

J. Am. Chem. Soc., **2004**, 126 (21), 6590-6598 • DOI: 10.1021/ja0393776 • Publication Date (Web): 28 April 2004

Downloaded from <http://pubs.acs.org> on March 31, 2009



More About This Article

Additional resources and features associated with this article are available within the HTML version:

- Supporting Information
- Links to the 6 articles that cite this article, as of the time of this article download
- Access to high resolution figures
- Links to articles and content related to this article
- Copyright permission to reproduce figures and/or text from this article

[View the Full Text HTML](#)

A Controlled Supramolecular Approach toward Cation-Specific Chemosensors: Alkaline Earth Metal Ion-Driven Exciton Signaling in Squaraine Tethered Podands

Easwaran Arunkumar, Parayali Chithra, and Ayyappanpillai Ajayaghosh*

Contribution from the Photosciences and Photonics Division, Regional Research Laboratory (CSIR), Trivandrum - 695019, India

Received November 2, 2003; E-mail: aajayaghosh@rediffmail.com

Abstract: Three different squaraine tethered bichromophoric podands **3a–c** with one, two, and three oxygen atoms in the podand chain and an analogous monochromophore **4a** were synthesized and characterized. Among these, the bichromophores **3a–c** showed high selectivity toward alkaline earth metal cations, particularly to Mg^{2+} and Ca^{2+} ions, whereas they were optically silent toward alkali metal ions. From the absorption and emission changes as well as from the Job plots, it is established that Mg^{2+} ions form 1:1 folded complexes with **3a** and **3b** whereas Ca^{2+} ions prefer to form 1:2 sandwich dimers. However, **3c** invariably forms weak 1:1 complexes with Mg^{2+} , Ca^{2+} , and Sr^{2+} ions. The signal output in all of these cases was achieved by the formation of a sharp blue-shifted absorption and strong quenching of the emission of **3a–c**. The signal transduction is achieved by the exciton interaction of the face-to-face stacked squaraine chromophores of the cation complex, which is a novel approach of specific cation sensing. The observed cation-induced changes in the optical properties are analogous to those of the “H” aggregates of squaraine dyes. Interestingly, a monochromophore **4a** despite its binding, as evident from 1H NMR studies, remained optically silent toward Mg^{2+} and Ca^{2+} ions. While the behavior of **4a** toward Mg^{2+} ion is understood, its optical silence toward Ca^{2+} ion is rationalized to the preferential formation of a “Head-Tail-Tail-Head” arrangement in which exciton coupling is not possible. The present study is different from other known reports on chemosensors in the sense that cation-specific supramolecular host–guest complexation has been exploited for controlling chromophore interaction via cation-steered exciton coupling as the mode of signaling.

Introduction

Supramolecular host–guest interaction and molecular recognition, particularly cation binding, is a subject of considerable interest due to its implications in many fields such as chemistry, biology, medicine, and environmental studies.¹ Such interactions will become useful when the host molecules are able to express the recognition event in the form of a measurable signal, invoking a change in one or more properties of the system such as redox potentials, absorption, or emission characteristics. The design of such molecular systems, chemosensors, the usual configuration of which consists of a macrocyclic receptor (ionophore) unit, integrated to an organic chromophore (fluorophore), is a topic of considerable interest.² Among various chemosensors, the design of cation-specific sensors for the selective detection of biologically important cations such as Na^+ , K^+ , Mg^{2+} , Ca^{2+} , and Zn^{2+} is of extreme importance.³ In this context, designing chemosensors for the specific recognition between alkali and alkaline earth metal cations is a challenging task.

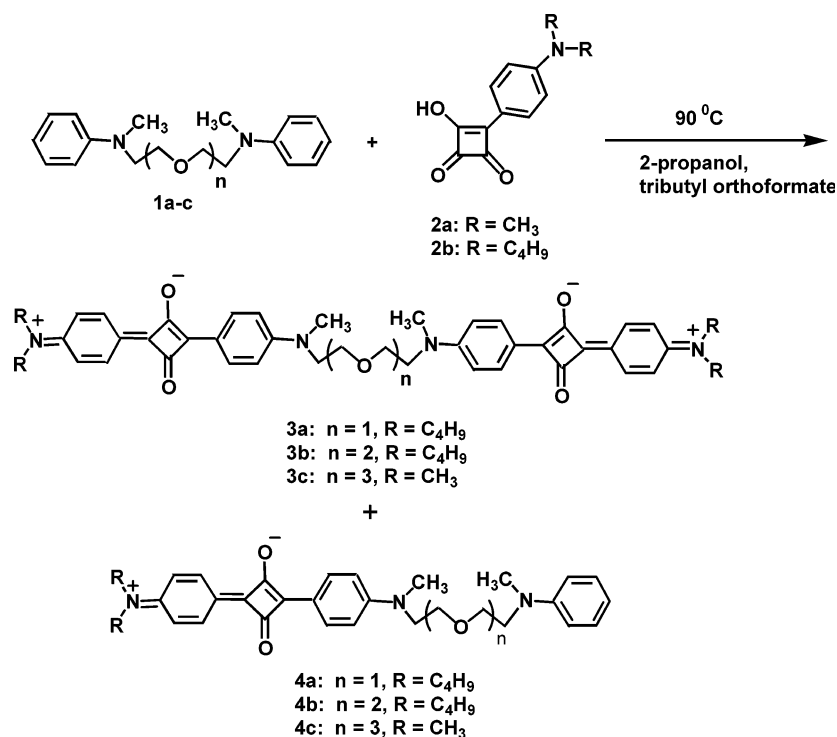
There are several reports in the literature which pertain to chemosensors that selectively detect alkaline earth metal ions.⁴ Even though macrocyclic receptors are the widely used cation binding sites in these systems, reports on chromophore-linked pseudomacrocyclic- or podand-based chemosensors are relatively few.^{5,6} For example, Nakamura et al. have reported several anthracene- or pyrene-linked podands, which specifically detect alkaline earth metal ions.⁶ In addition, there are a few recent

(1) (a) Lehn, J.-M. *Supramolecular Chemistry Concepts and Perspectives*; Wiley-VCH: Weinheim, 1995. (b) Gokel, G. W. Molecular recognition for cationic guests. In *Comprehensive Supramolecular Chemistry*; Gokel, G. W., Ed.; Elsevier Science: Oxford, 1996; Vol. 1. (c) Steed, J. W.; Atwood, J. L. *Supramolecular Chemistry*; John Wiley & Sons, Ltd.: England, 2000.

(2) (a) Valeur, B. In *Molecular Luminescence Spectroscopy: Part 3*; Schulman, S. G., Ed.; Wiley: New York, 1993. (b) Valeur, B. In *Topics in Fluorescence Spectroscopy*; Lakowicz, J. R., Ed.; Plenum Press: New York, 1994; Vol. 4. (c) Valeur, B.; Badaoui, F.; Bardez, E.; Bourson, J.; Boutin, P.; Chatelain, A.; Devol, I.; Larrey, B.; Lefevre, J. P.; Soulet, A. In *Chemosensors of Ion and Molecular Recognition*; Desvergne, J.-P., Czarnik, A. W., Eds.; NATO ASI Series; Kluwer: Dordrecht, 1997. (d) Fabbrizzi, L.; Poggi, A. *Chem. Soc. Rev.* **1995**, 197. (e) de Silva, A. P.; Gunaratne, H. Q. N.; Gunnlaugsson, T.; Huxley, A. J. M.; McCoy, C. P.; Rademacher, J. T.; Rice, T. E. *Chem. Rev.* **1997**, 97, 1515. (f) Valeur, B.; Leray, I. *Coord. Chem. Rev.* **2000**, 205, 3. (g) McQuade, D. T.; Pullen, A. E.; Swager, T. M. *Chem. Rev.* **2000**, 100, 2537.

(3) (a) de Silva, A. P.; Gunaratne, H. Q. N.; McCoy, C. P. *Nature* **1993**, 364, 42. (b) Grandini, P.; Mancin, F.; Tecilla, P.; Scrimin, P.; Tonellato, U. *Angew. Chem., Int. Ed.* **1999**, 38, 3061. (c) Prodi, L.; Bargossi, C.; Montalti, M.; Zaccaroni, N.; Su, N.; Bradshaw, J. S.; Izatt, R. M.; Savage, P. B. *J. Am. Chem. Soc.* **2000**, 122, 6769. (d) Hirano, T.; Kikuchi, K.; Urano, Y.; Higuchi, T.; Nagano, T. *J. Am. Chem. Soc.* **2000**, 122, 12399. (e) de Silva, S. A.; Amorelli, B.; Isidor, D. C.; Loo, K. C.; Crooker, K. E.; Pena, Y. E. *Chem. Commun.* **2002**, 1360. (f) Shin, E. J. *Chem. Lett.* **2002**, 686. (g) de Silva, A. P.; McClean, G. D.; Pagliari, S. *Chem. Commun.* **2003**, 2010. (h) Wu, K.-C.; Ahmed, M. O.; Chen, C.-Y.; Huang, G.-W.; Hon, Y.-S.; Chou, P.-T. *Chem. Commun.* **2003**, 890.

Scheme 1



cently, Liang et al. have reported that squaraines, which are linked to flexible alkyl chains in a bichromophoric fashion, show exciton coupled spectral changes, depending upon the length of the alkyl chain.²⁰ However, this property of squaraine dyes has never before been exploited in the designing of chemosensors, until recently when we reported the Ca²⁺ ion-specific exciton interaction in a squaraine foldamer.²¹ In the present study, we illustrate a supramolecular approach in combination with cation-driven exciton interaction for the signaling of a specific cation binding, where the mode of complexation and chromophore interaction are controlled by the nature of the host and guest molecules.

Results and Discussion

Synthesis and Characterization of Squaraine Bichromophores 3a–c and the Monochromophore 4a. The bis-aniline derivatives **1a–c** and the squaric acid derivatives **2a** and **2b** were prepared as per reported procedures.^{22,23} Reaction of **1a–c** with the semisquaraine derivative **2a** or **2b** in a 1:2 stoichiometry, under reflux conditions in 2-propanol using tributyl orthoformate as catalyst, resulted in the formation of the bichromophores **3a–c** in 20–25% yields along with small amounts of the monochromophores **4a–c** (Scheme 1). In a separate experiment, the monochromophore **4a** was synthesized in 32% yield by a controlled reaction between **1a** and **2b** in a 1:1 stoichiometry. FT-IR spectra of **3a–c** and **4a** showed a sharp band at 1590 cm⁻¹, characteristic of the C–O⁻ stretching of the zwitterionic squaraine dyes. ¹H NMR spectra of **3a–c** in CDCl₃ showed resonance signals corresponding to –NCH₃, –OCH₂, and –NCH₂ protons at δ 3.1, 3.54, and 3.65 ppm,

Table 1. Absorption and Emission Parameters for Compounds **3a–c** and **4a** in Acetonitrile

compound	absorption		emission ^a	
	λ _{max} (nm)	ε (M ⁻¹ cm ⁻¹)	λ _{max} (nm)	Φ _f ^b
3a	652	120 226	664	0.008
	618			
	587 (sh)			
3b	644	134 896	663	0.014
	625			
	630			
3c	630	138 038	654	0.023
4a	637	229 086	664	0.06

^a Solutions were excited at 570 nm, and emission was monitored in the region 600–750 nm for estimating Φ_f. ^b Fluorescence quantum yields were determined using 4,4-[bis-(*N,N*-dimethylamino)phenyl]squaraine dye as the standard (Φ_f = 0.7 in CHCl₃), error limit ±5%.

respectively. Due to the symmetry of the charge-delocalized zwitterionic structures of **3a–c**, the aromatic protons appeared as two sets of four protons each at δ 6.7 and 8.3 ppm. The ¹H NMR spectrum of **4a** in CDCl₃ showed two characteristic singlets at δ 3.1 and 2.86 ppm, corresponding to three protons each of the two –NCH₃ groups. The –NCH₂ and –OCH₂ protons appeared as multiplets around δ 3.5–3.75 ppm. In the aromatic region, five different signals could be seen. Signals at δ 8.2 and 6.7 ppm, which correspond to four protons, are assigned to the squaraine moiety. Signals at δ 7.2 and 6.7 ppm, corresponding to two protons each, and the signal at δ 6.6 ppm corresponding to a single proton are assigned to the aniline moiety. ¹³C NMR spectra of **3a–c** and **4a**, high-resolution mass spectra, and the elemental analyses data were in agreement with their assigned structures. The high-resolution mass spectra of **3a–c** showed the characteristic [M]⁺ ion peak, whereas the MALDI-TOF mass spectra showed the [M + H]⁺ ion peak along with [M + Na]⁺ and [M + K]⁺ peaks.

Absorption and Emission Properties of 3a–c and 4a. The absorption and emission maxima and the fluorescence quantum

(20) Liang, K.; Farahat, M. S.; Perlstein, J.; Law, K.-Y.; Whitten, D. G. *J. Am. Chem. Soc.* **1997**, *119*, 830.

(21) Ajayaghosh, A.; Arunkumar, E.; Daub, J. *Angew. Chem., Int. Ed.* **2002**, *41*, 1766.

(22) Robello, D. R. *J. Polym. Sci., Part A: Polym. Chem.* **1990**, *28*, 1.

(23) Keil, D.; Hartmann, H. *Dyes Pigm.* **2001**, *49*, 161.

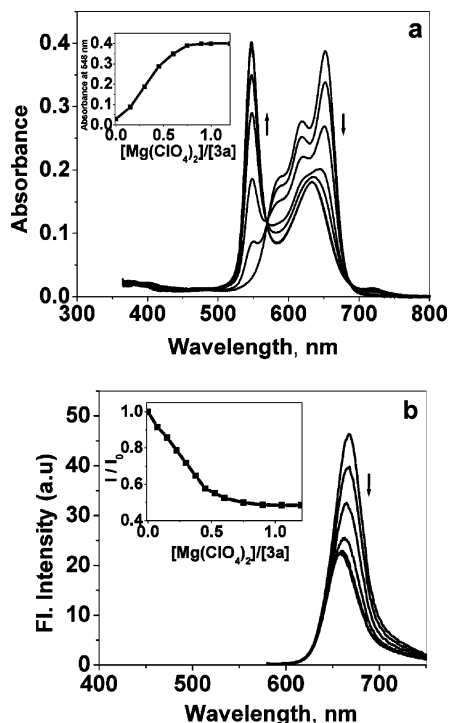


Figure 2. Changes in the (a) absorption and (b) emission spectra of **3a** ($3.6 \mu\text{M}$) in acetonitrile with the addition of $\text{Mg}(\text{ClO}_4)_2$. The arrows indicate the changes that result from progressively increasing the concentration of $\text{Mg}(\text{ClO}_4)_2$. Insets show variation of (a) absorbance at 548 nm and (b) fluorescence intensity at 664 upon increasing the ratio $[\text{Mg}(\text{ClO}_4)_2]/[\mathbf{3a}]$.

yields of **3a–c** and **4a** in acetonitrile are presented in Table 1. The bichromophore **3a** showed an intense absorption maximum at 652 nm with two strong shoulders around 620 and 585 nm (Figure 2a). The fluorescence emission spectrum of **3a** in acetonitrile ($3.6 \times 10^{-6} \text{ M}$) showed a maximum at 664 nm with a low quantum yield of 0.008 (Figure 2b). The absorption spectrum of **3b** having two oxygen atoms in the podand chain exhibited two close maxima at 644 and 625 nm with a weak shoulder around 590 nm. The emission maximum of **3b** was at 663 nm with a quantum yield of 0.014. Interestingly, **3c** showed a sharp spectrum with absorption maximum at 630 nm and an emission maximum at 654 nm. The fluorescence quantum yield of **3c** is 0.023, which is higher than those of **3a** and **3b**. The absorption and emission maxima of **4a** in acetonitrile occurred at 637 and 664 nm, respectively, with a fluorescence emission quantum yield of 0.06, which is almost 8 times higher than that of **3a**. The differences in the spectral pattern and the quantum yields of **3a–c** are attributed to the oxyethylene chain-dependent chromophore interaction, in analogy to the report by Liang et al.²⁰

Cation Binding Properties of 3a–c: Changes in the Absorption and Emission Spectra. Changes in the absorption and emission spectra of **3a** in acetonitrile ($3.6 \times 10^{-6} \text{ M}$) upon the addition of aliquots of $\text{Mg}(\text{ClO}_4)_2$ are shown in Figure 2. With an increasing amount of $\text{Mg}(\text{ClO}_4)_2$, the intensity of the absorption maximum at 652 nm is decreased with the concomitant growth of a new sharp band at 548 nm, through an isosbestic point at 570 nm. The inset of Figure 2a shows a plot of the absorbance at 548 nm against the ratio of the concentrations of $\text{Mg}(\text{ClO}_4)_2$ and **3a**, which gets saturated when the concentration of the metal salt equals that of **3a** indicating a 1:1 complexation

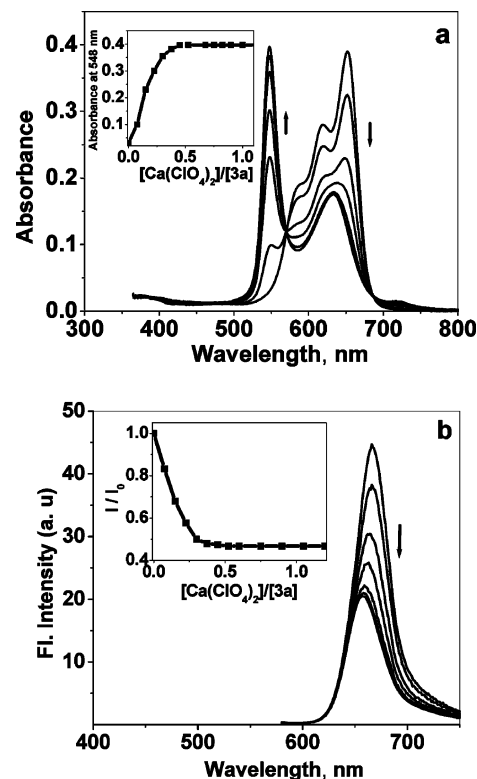


Figure 3. Changes in (a) absorption and (b) emission spectra of **3a** ($3.6 \mu\text{M}$) in acetonitrile with the addition of $\text{Ca}(\text{ClO}_4)_2$. The arrows indicate the changes that result from progressively increasing the concentration of $\text{Ca}(\text{ClO}_4)_2$. Insets show variation of (a) absorbance at 548 nm and (b) fluorescence intensity at 664 nm with the ratio $[\text{Ca}(\text{ClO}_4)_2]/[\mathbf{3a}]$.

between the two. Similarly, upon addition of $\text{Mg}(\text{ClO}_4)_2$, the intensity of the emission band at 664 nm ($\Phi_f = 0.008$) gradually decreased with a marginal blue-shift (8 nm) when excited at 570 nm (Figure 2b). The quenching of the emission gets saturated ($\Phi_f = 0.004$) when the concentration of $\text{Mg}(\text{ClO}_4)_2$ reached nearly that of **3a**, indicating a 1:1 stoichiometry of binding (Figure 2b, inset).

Changes in the absorption and emission spectra of **3a** ($3.6 \times 10^{-6} \text{ M}$) induced by the addition of $\text{Ca}(\text{ClO}_4)_2$ in acetonitrile are shown in Figure 3, which are identical as in the case of $\text{Mg}(\text{ClO}_4)_2$. However, in the case of $\text{Ca}(\text{ClO}_4)_2$, the plot of absorbance at 548 nm reached a maximum when the ratio of the concentrations of the metal salt and **3a** reached a value of 0.5 (Figure 3a, inset). A same effect is observed when the ratio of the fluorescence intensities (I/I_0) was plotted against the ratio of concentration of $\text{Ca}(\text{ClO}_4)_2$ and **3a**, indicating a 2:1 stoichiometry for the complexation of **3a** with Ca^{2+} ion. Similar changes in the absorption and emission spectra could be obtained when $\text{Sr}(\text{ClO}_4)_2$ was added to an acetonitrile solution of **3a**. However, addition of $\text{Ba}(\text{ClO}_4)_2$ to **3a** showed weak changes, indicating a very loose interaction between the two. Interestingly, addition of LiClO_4 , NaClO_4 , and KClO_4 did not induce any change in the absorption or emission properties of **3a**, revealing its high specificity toward alkaline earth metal cations. These observations are justified by a comparison of the plots of the fluorescence quantum yields (Φ_f) against the ratio of the concentrations of metal salt to the bichromophore **3a** (Figure 4).

To determine the role of the podand chain length on the cation sensing properties, the bichromophores **3b** and **3c** were subjected to detailed metal ion titration studies. Changes in the absorption

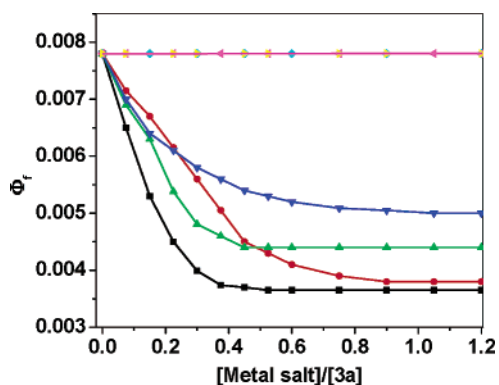


Figure 4. Plot of Φ_f versus the ratio of [metal salt] to [3a] illustrating the variation of fluorescence quantum yield of the bichromophore with various metal cations such as Ca^{2+} (■), Mg^{2+} (●), Sr^{2+} (▲), Ba^{2+} (▼), Na^+ (◆), K^+ (▲), and Li^+ (◆).

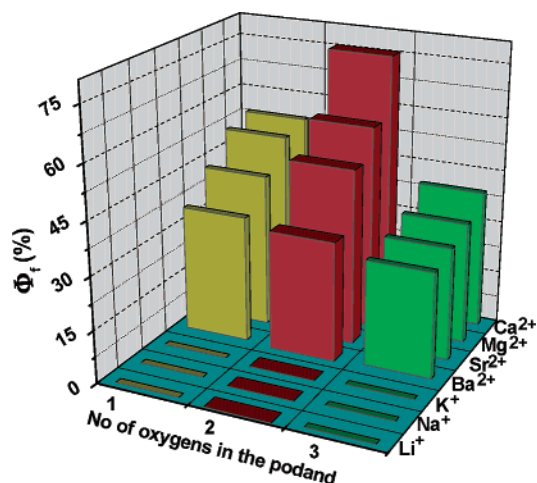


Figure 5. A 3D plot showing the selectivity and sensitivity of **3a–c** toward various metal cations.

and emission spectra of **3b** upon gradual addition of $\text{Mg}(\text{ClO}_4)_2$ and $\text{Ca}(\text{ClO}_4)_2$ are presented in the Supporting Information. Although these changes of **3b** are similar to those of **3a**, the former showed better selectivity and sensitivity toward Ca^{2+} ion. Addition of $\text{Sr}(\text{ClO}_4)_2$ and $\text{Ba}(\text{ClO}_4)_2$ showed weak response, whereas LiClO_4 , NaClO_4 , and KClO_4 had hardly any effect. The bichromophore **3b** also formed a 1:1 complex with Mg^{2+} , whereas Ca^{2+} and Sr^{2+} ions showed a 1:2 complexation mode as in the case of **3a**. In contrast to the behavior of **3a** and **3b**, the bichromophore **3c** having a long podand chain (three oxygen atoms) invariably showed a 1:1 binding with $\text{Mg}(\text{ClO}_4)_2$, $\text{Ca}(\text{ClO}_4)_2$, and $\text{Sr}(\text{ClO}_4)_2$. However, in these cases, the response toward the metal cations was relatively weaker when compared to those of **3a** and **3b**. A 3D plot of the percentage of fluorescence quantum yields of **3a–c** against various metal cations reveals the effect of the podand chain on the selectivity and sensitivity on cation binding (Figure 5). From the fluorescence quenching data, the maximum sensitivity and selectivity are obtained for **3b**. In all cases, the sensitivity was in the order $\text{Ca}^{2+} > \text{Mg}^{2+} > \text{Sr}^{2+} > \text{Ba}^{2+}$.

The difference in the complexation modes of **3a–c** with Mg^{2+} and Ca^{2+} was confirmed by the corresponding Job plots.^{24,25} For example, the Job plots of **3a** with Mg^{2+} and Ca^{2+} ions are

shown in Figure 6. In the case of Mg^{2+} binding, the maximum absorbance of the complex is obtained when the mole fraction of the host (**3a**) has reached 0.5, which is a signature of a 1:1 stoichiometry (Figure 6a). However, for Ca^{2+} , the maximum absorbance at 548 nm could be seen when the mole fraction of **3a** was at 0.66, which is characteristic of a host–guest binding in a 2:1 stoichiometry (Figure 6b). Similar results were obtained for **3b**. The Benesi–Hildebrand²⁶ plot for Mg^{2+} binding showed a good linear relationship of a 1:1 complexation with a binding constant of $6.15 \times 10^5 \text{ M}^{-1}$ for **3a** and $1.04 \times 10^6 \text{ M}^{-1}$ for **3b**. It must be noted here that in acetonitrile ($\epsilon = 38.8$) ambiguity exists regarding the complete dissociation of the metal salts. However, for bivalent metal cations in micromolar concentrations, we assume the complete dissociation of the metal salts and the resultant complexes are not ion paired.²⁷

¹H NMR Binding Studies of 3a with $\text{Ca}(\text{ClO}_4)_2$ and $\text{Mg}(\text{ClO}_4)_2$. The effect of the addition of $\text{Mg}(\text{ClO}_4)_2$ and $\text{Ca}(\text{ClO}_4)_2$ to the ¹H NMR spectrum of **3a** in a mixture of 30% CD_3CN and 70% CDCl_3 is shown in Figure 7. After the addition of an equivalent amount of $\text{Mg}(\text{ClO}_4)_2$ or $\text{Ca}(\text{ClO}_4)_2$, the well-resolved resonance signals of **3a** (Figure 7a) became broad and shifted toward upfield. For example, the signals at δ 8.3 and 6.8 ppm, which correspond to the squaraine aromatic protons, became very broad between δ 7.7–9.0 and δ 5.5–7.0 ppm, respectively. Similarly, signals corresponding to $-\text{NCH}_3$, $-\text{OCH}_2$, and $-\text{NCH}_2-$ protons at δ 3.1, 3.54, and 3.65 ppm, respectively, were shifted toward lower δ values and merged to form broad signals. A considerable shift could also be noticed for the water signal at δ 2.1 ppm, toward low field after the addition of metal perchlorates, indicating the involvements of water molecules in the metal ion coordination processes. Interestingly, addition of LiClO_4 , NaClO_4 , or KClO_4 to **3a** did not show any change in the NMR spectrum, revealing no interaction between these cations with **3a**, which is in agreement with the absorption and emission spectral studies.

Exciton Coupled Signaling of the Cation Binding Events.

From the detailed analysis of the changes in the absorption and emission properties, and from the Job plots, it is clear that **3a** and **3b** form 1:1 complexes with Mg^{2+} ion whereas Ca^{2+} and Sr^{2+} ions prefer to form 1:2 complexes (Schemes 2 and 3). Mg^{2+} ion induces the folding of **3a** to form a foldamer, **5**, in a 1:1 stoichiometry, whereas Ca^{2+} ion prefers to form a 1:2 sandwich dimer, **6**, with **3a**. The difference in the absorption and emission properties of the cation complexes **5** and **6** from that of **3a** can be rationalized on the basis of the exciton interaction in the face-to-face stacked squaraine chromophores of the former. It is interesting to mention here that the cation-induced changes in the optical properties of **3a–c** are similar to those of the “H” aggregates of analogous squaraine dyes.¹⁹

In analogy to the exciton theory of dye aggregation, the cation-induced folding or dimerization of **3a–c** results in the splitting of the excited-state energy levels of the complex into two, one of which is higher in energy and the other lower in

(24) (a) Job, P. *Ann. Chem.* **1928**, *9*, 113. (b) Gil, V. M. S.; Oliveira, N. C. J. *Chem. Educ.* **1990**, *67*, 473.

(25) A Job plot is extensively used to find the complexation mode of the host–guest interaction. For examples, see: (a) Specht, A.; Bernard, P.; Goeldner, M.; Peng, L. *Angew. Chem., Int. Ed.* **2002**, *41*, 4706. (b) Huang, F.; Gibson, H. W.; Bryant, W. S.; Nagvekar, D. S.; Fronczek, F. R. *J. Am. Chem. Soc.* **2003**, *125*, 9367. (c) Huang, F.; Fronczek, F. R.; Gibson, H. W. *Chem. Commun.* **2003**, 1480.

(26) Benesi, H. A.; Hildebrand, J. H. *J. Am. Chem. Soc.* **1949**, *71*, 2703.

(27) We thank an anonymous reviewer for the comments on salt dissociation and ion pairing. The reported binding constants are based on the assumption that the concentration of the free ions is equal to the total salt concentration.

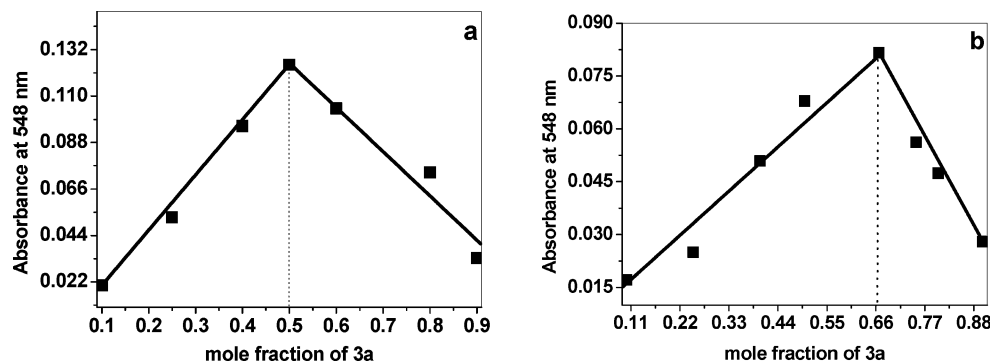


Figure 6. Job plots for the binding of **3a** with Mg²⁺ and Ca²⁺ ions: (a) 1:1 complexation with Mg²⁺; (b) 2:1 complexation with Ca²⁺.

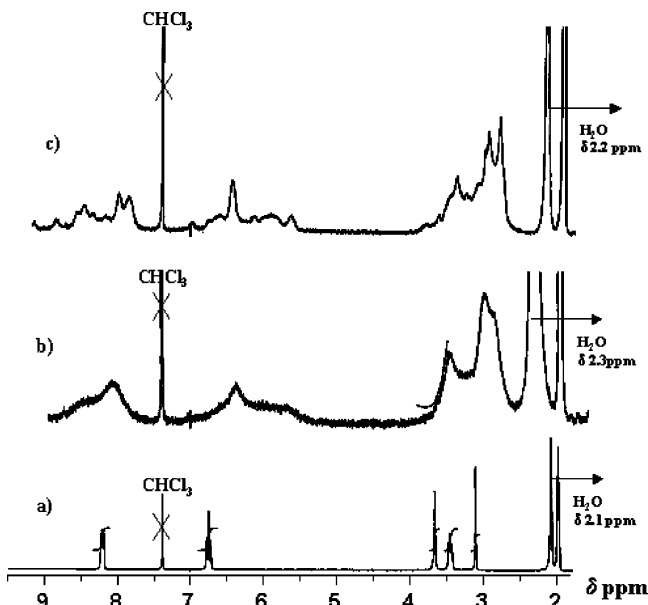


Figure 7. ¹H NMR spectra in 30% CD₃CN–70% CDCl₃ of **3a** (a) before addition of metal perchlorates (2.3 mM), (b) with 2.3 mM Mg(ClO₄)₂, and (c) with 2.3 mM Ca(ClO₄)₂.

energy.²⁸ The spectral shift ($\Delta\nu$) associated with the electronic transition in such cases will be determined by the tilt angle α of the transition dipole moments of the cation-complexed chromophores with the line of centers, which is given by the equation,

$$\Delta\nu (\text{dimer}) = h^{-1} \langle m^2 \rangle (1 - 3 \cos^2 \alpha) / r^2 \quad (1)$$

where h is Planck's constant, r is the separation of the molecular centers, and $\langle m^2 \rangle$ is the dipole moment of the dye monomer.²⁹ From this relationship, it can be seen that when α becomes greater than 54°44', the value of $\Delta\nu$ changes to positive, indicating a hypsochromic shift, and reaches a maximum when α becomes 90°. In the case of the folded complex **5** and the sandwich dimer **6**, the squaraine chromophores are face-to-face stacked as in the case of "H" aggregates where α tends to approach 90°. As a result, the excited state of the complex will

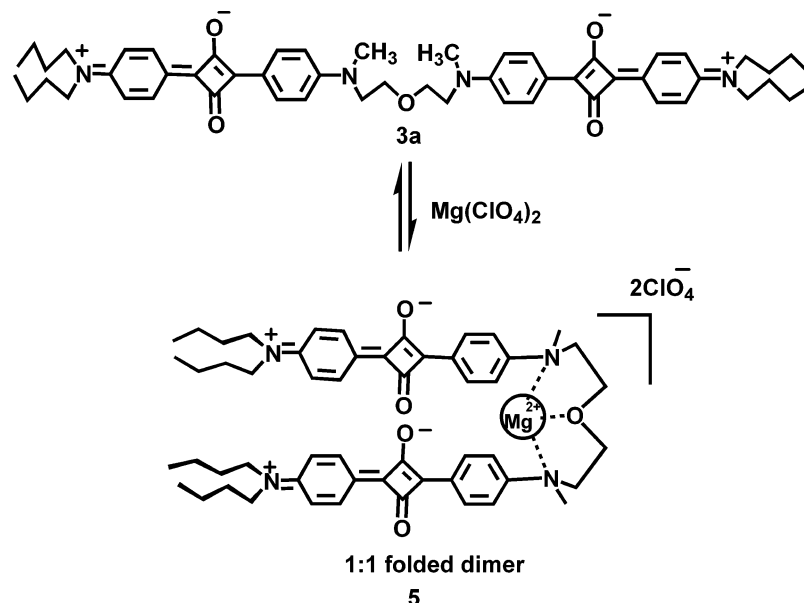
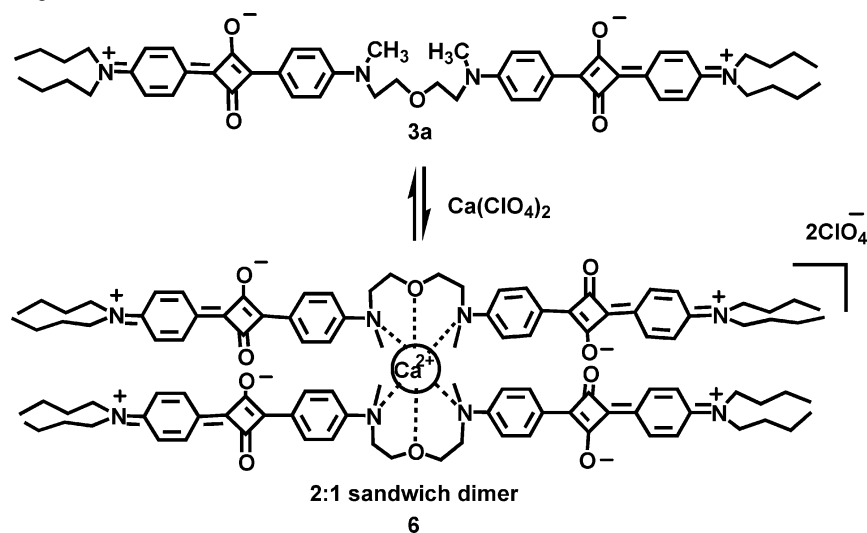
be shifted to higher energy, resulting in a blue-shifted absorption. Consequently, the emission of the bound complexes is weak because the internal conversion from the upper excited state to the lower one is very fast and the emission from the lower excited state is theoretically forbidden.

Cation Binding Property of the Monochromophore **4a**.

In light of the cation binding behavior of the bichromophores **3a–c**, we speculated that a monochromophore **4a** might be able to distinguish between Mg²⁺ and Ca²⁺ ions. The rationale for this speculation was that signaling would not be possible in the 1:1 folded complex of **4a** with Mg²⁺ where exciton coupling is not possible. However, signaling will be possible in a 1:2 complex of **4a** with Ca²⁺, in the event of a face-to-face stacking of the squaraine chromophore. However, **4a** was optically silent toward both Mg²⁺ and Ca²⁺ ions. While this is understood for Mg²⁺ ions, the silence of Ca²⁺ ions against **4a** was surprising, which is rationalized by considering the two statistical complexation modes of **4a** with Ca²⁺ ions as shown in Scheme 4. The "Head-Tail-Head-Tail" (H-T-H-T) arrangement **7** is expected to give an exciton coupled blue-shifted spectrum with Ca²⁺ ion, whereas the "Head-Tail-Tail-Head" (H-T-T-H) arrangement **8** should be optically silent. Because the absorption or emission spectra of **4a** did not change upon addition of Ca(ClO₄)₂, it is reasonable to assign the "H-T-T-H" assembly **8** for the 2:1 complex of **4a** with Ca²⁺ ion in which the two squaraine chromophores are positioned away from each other, thereby preventing exciton interaction between the chromophores.

In the context of the above observations, it is important to see that **4a** is optically silent toward Mg²⁺ and Ca²⁺ ions despite their binding to **4a**. This is proved by the ¹H NMR studies of **4a** in CD₃CN in the presence of Mg²⁺ and Ca²⁺ ions (Figure 8). In both cases, considerable changes to the resonance signals could be noticed upon addition of the metal perchlorates. Signals corresponding to the aromatic protons of the squaraine moiety at δ 6.87 and δ 8.2 ppm became broad and weak. The signal at δ 3.1 ppm corresponding to the N–CH₃ protons, attached to the squaraine moiety, is shifted upfield and merged with the N–CH₃ protons of the aniline moiety, which appeared at δ 2.86 ppm. The multiplets at δ 3.44–3.65 ppm corresponding to the –OCH₂ and –NCH₂ protons underwent considerable shift toward high field, particularly the –NCH₂ protons. It is interesting to note that the resonance signals at δ 6.6–6.68 and δ 7.14 ppm, which correspond to the aromatic protons of the aniline moiety of **4a**, did not show many changes in the presence of Ca(ClO₄)₂ whereas addition of Mg(ClO₄)₂ induced consider-

(28) (a) Kasha, M.; Rawls, H. R.; El-Bayoumi, M. A. *Pure Appl. Chem.* **1965**, *11*, 371. (b) Davydov, A. S. *Theory of Molecular Excitons*; Plenum Press: New York, 1971. (c) McRae, E. G.; Kasha, M. *Physical Process in Radiation Biology*; Academic Press: New York, 1964; p 17. (d) Hochstrasser, R. M.; Kasha, M. *Photochem. Photobiol.* **1964**, *3*, 317. (e) Czikkely, V.; Forsterling, H.; Kuhn, H. *Chem. Phys. Lett.* **1970**, *6*, 11. (f) Bucher, H.; Kuhn, H. *Chem. Phys. Lett.* **1970**, *6*, 183.
(29) Emerson, E. S.; Conlin, M. A.; Rosenoff, A. E.; Norland, K. S.; Rodriguez, H.; Chin, D.; Bird, G. R. *J. Phys. Chem.* **1967**, *71*, 2396.

Scheme 2. Mg²⁺ Ion Induced Folding of **3a** to a 1:1 Folded Dimer**Scheme 3.** Ca²⁺ Ion Binding of **3a** To Form a 2:1 Sandwich Dimer

able broadening. These observations indicate that, in the 1:1 folded complex of **4a** with Mg²⁺, the aniline moiety experiences considerable interaction with the squaraine moiety whereas in the case of the “H-T-T-H” sandwich dimer of **4a** with Ca²⁺, the aniline moieties seem to be slightly displaced from the squaraine chromophore. Thus, while the NMR experiments clearly support the binding of Ca²⁺ to **4a**, the absorption and emission studies strongly favor the “H-T-T-H” arrangement for the complex where there is no possibility for exciton interaction as shown in Scheme 4, which justify its optical silence toward the Ca²⁺ ion.

Conclusions

In the present study, we have illustrated a rational supramolecular approach in controlling and expressing the binding of specific cations, invoking exciton interaction as the mode of optical signaling, which is different from other known signaling mechanisms. The results obtained from the absorption, emission, and ¹H NMR studies revealed the difference in the supramolecular control of the binding modes of the bichromophores

3a–c and the monochromophore **4a** with Mg²⁺ and Ca²⁺ ions. From the absorption and emission changes and from the Job plots, it is clear that **3a** and **3b** bind with Mg²⁺ ion to form intramolecular 1:1 foldamers whereas Ca²⁺ ion prefers to bind in a 1:2 stoichiometry leading to intermolecular sandwich dimers. However, the bichromophore **3c** invariably forms 1:1 folded complexes with Mg²⁺ and Ca²⁺ ions. However, addition of LiClO₄, NaClO₄, or KClO₄ did not bring any difference in the absorption or emission properties of **3a–c**, making them selective toward alkaline earth metal ions. Interestingly, the monochromophore **4a** is optically silent toward Mg²⁺ and Ca²⁺ ions. While this is clear in the case of Mg²⁺ ion, the optical silence of **4a** toward Ca²⁺ ion is rationalized on the basis of the preferential complexation in a “H-T-T-H” arrangement where exciton coupling of the chromophore is not allowed. The present study is different from other reports on chemosensors in the sense that the cation-specific supramolecular host–guest interaction has been exploited for controlling and expressing ion recognition via chromophore interaction, which in turn

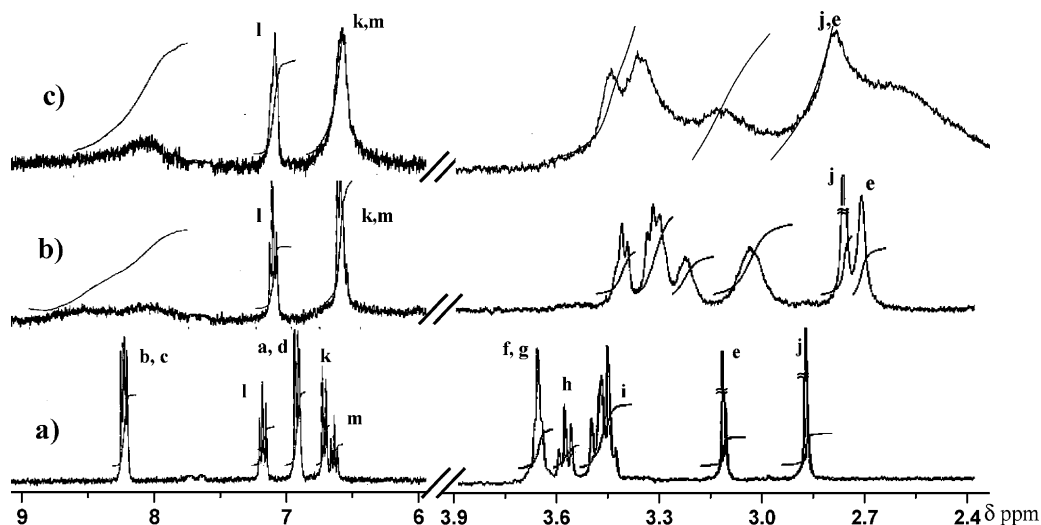
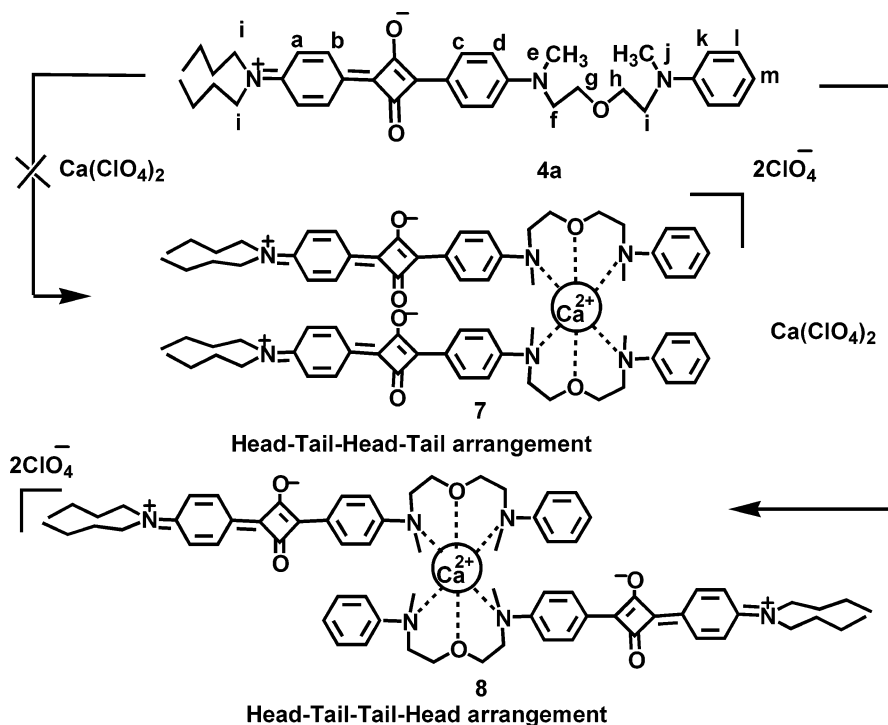


Figure 8. ^1H NMR spectral changes (300 MHz, 300 K) of **4a** (3.52 mM) in CD_3CN (a) before addition of metal perchlorates, (b) after addition of $\text{Ca}(\text{ClO}_4)_2$ (3.52 mM), and (c) after addition of $\text{Mg}(\text{ClO}_4)_2$ (3.52 mM).

Scheme 4. Possible Complexation Modes of **4a** with $\text{Ca}(\text{ClO}_4)_2$



becomes the key process in the signal transduction. The present approach successfully could translate changes in the photo-physical properties associated with a dye aggregation to a measurable signal, making use of the cation-specific supramolecular organization of chromophore-linked podands. In addition, the present study demonstrates how organic dye aggregation, a well-studied phenomenon with respect to organic semiconducting devices³⁰ and supramolecular chemistry,³¹ becomes important in the design of cation selective chemosensors.

Experimental Section

Unless otherwise stated, all starting materials and reagents were purchased from commercial suppliers and used without further purification. The solvents used were purified and dried by standard methods prior to use. Melting points were determined with a Mel-Temp-II melting point apparatus and are uncorrected. FT-IR spectra were

recorded on a Nicolet Impact 400D infrared spectrophotometer. ^1H and ^{13}C NMR spectra were measured on a 300 MHz Bruker Avance DPX spectrometer using TMS as internal standard. High-resolution mass spectra were recorded in a Finnigan MAT 95 instrument using xenon as ionization gas. Matrix-assisted laser desorption ionization time-of-flight (MALDI-TOF) mass spectra were obtained on a Perseptive Biosystems Voyager DE-Pro MALDI-TOF mass spectrometer. Elemental analyses were done using a Perkin-Elmer series-II 2400 CHN analyzer. The emission spectra were measured on a Spex-Fluorolog F112X spectrofluorimeter. Fluorescence quantum yields were determined in spectroscopic grade CH_3CN using optically matching solutions

- (30) Zollinger, H. *Color Chemistry. Synthesis, Properties and Applications of Organic Dyes and Pigments*; VCH: Weinheim, 1991.
 (31) (a) Würthner, F.; Yao, S. *Angew. Chem., Int. Ed.* **2000**, *39*, 1978. (b) Würthner, F.; Yao, S.; Beginn, U. *Angew. Chem., Int. Ed.* **2003**, *42*, 3247. (c) Würthner, F.; Yao, S.; Debaerdemaeker, T.; Wortmann, R. *J. Am. Chem. Soc.* **2002**, *124*, 9431 and references therein.

of 4,4-[bis-(*N,N*-dimethylamino)phenyl]-squaraine dye ($\Phi_F = 0.70$ in chloroform) as standard. The stability constants (K_s) were determined from the absorption spectral changes using the equation,

$$\frac{A_0}{(A_0 - A)} = \frac{\epsilon_L}{\epsilon_L - \epsilon_{ML}} \left(\frac{1}{K_s[M]} + 1 \right)$$

where ϵ_L and ϵ_{ML} are the molar extinction coefficients of the ligand and the complex, respectively. The quantity $A_0/(A_0 - A)$ is plotted versus $1/[M]$, and the stability constant is then obtained from the ratio intercept/slope.

General Procedure for the Metal Ion Binding Studies. Metal perchlorate solutions were prepared in spectroscopic grade acetonitrile. The bichromophores **3a–c** were dissolved in acetonitrile under sonication and warming in a water bath. Metal ion titrations were carried out by adding small volumes (1–5 μ L) of the metal salt solutions (10^{-6} M in CH_3CN , 4 mL) in a quartz cuvette. After the addition of metal perchlorate solution to the cuvette using a microliter syringe, the solution was shaken well and was left to stand for 1 min before recording the absorption and emission spectra of the metal complexed dye.

General Procedure for the Preparation of the Bichromophores 3a–c. To a 100 mL round-bottomed flask containing 50 mL of 2-propanol were added the appropriate bisaniline derivative (0.35 mmol), *N,N*-(dialkylamino)phenyl-4-hydroxy cyclobut-3-ene-1,2-dione (0.86 mmol), and tributyl orthoformate (1 mL). The reaction mixture was then refluxed for 20 h. The hot reaction mixture was filtered, and the solid was washed with 2-propanol until the filtrate was almost colorless. Column chromatography (chloroform/methanol, 9:1) of the crude product over silica gel (100–200 mesh) gave the pure product. Yields, melting points, and spectral details of each product are given below.

3a. Yield: 25%. mp 230–232 °C. FT-IR (KBr): $\nu = 1590, 1481, 1398, 1351, 1175, 1113, 984, 917, 839, 787 \text{ cm}^{-1}$. $^1\text{H NMR}$ (300 MHz, CDCl_3 , TMS): δ 0.96–1.01 (t, $J = 7.28 \text{ Hz}$, 12H, $-\text{CH}_3$), 1.36–1.6 (m, 16H, $-\text{CH}_2$), 3.10 (s, 6H, $-\text{NCH}_3$), 3.41–3.46 (m, 8H, $-\text{NCH}_2$), 3.65–3.67 (m, 8H, $-\text{NCH}_2$, $-\text{OCH}_2$), 6.70–6.77 (dd, $J = 1.23, 9.3 \text{ Hz}$, 8H, aromatic), 8.35–8.39 (dd, $J = 2.4, 9.2 \text{ Hz}$, 8H, aromatic) ppm. $^{13}\text{C NMR}$ (75 MHz, CDCl_3): δ 13.8, 20.2, 29.6, 39.5, 51.2, 52.3, 69, 112.3, 112.4, 119.5, 120.2, 132.8, 133.6, 153.8, 183.3, 187.5, 189.3 ppm. HRMS-FAB: $[\text{M}]^+$ calcd for $\text{C}_{54}\text{H}_{66}\text{N}_4\text{O}_5$, 851.5111; found, 851.5103.

3b. Yield: 27%. mp 236–238 °C. FT-IR (KBr): $\nu = 1589, 1460, 1390, 1367, 1181, 1129, 875 \text{ cm}^{-1}$. $^1\text{H NMR}$ (300 MHz, CDCl_3 , TMS): δ 0.907–0.99 (t, $J = 7.27 \text{ Hz}$, 12H, $-\text{CH}_3$), 1.37–1.63 (m, 16H, $-\text{CH}_2$), 3.14 (s, 6H, $-\text{NCH}_3$), 3.42–3.64 (m, 20H, $-\text{NCH}_2$, and $-\text{OCH}_2$), 6.69–6.77 (dd, $J = 1.4, 9.32 \text{ Hz}$, 8H, aromatic), 8.33–8.36 (dd, $J = 2.3, 9.25 \text{ Hz}$, 8H, aromatic) ppm. $^{13}\text{C NMR}$ (75 MHz, CDCl_3): δ 13.8, 20.2, 29.4, 39.5, 51.2, 52.3, 68.7, 70.93, 112.4, 112.9, 119.5, 120, 132.8, 133.5, 153.8, 183.4, 187.6, 189.2 ppm. Anal. Calcd for $\text{C}_{56}\text{H}_{70}\text{N}_4\text{O}_6$: C, 75.14; H, 7.88; N, 6.26. Found: C, 74.96; H, 7.96;

N, 6.10. HRMS-FAB: $[\text{M}]^+$ calcd for $\text{C}_{56}\text{H}_{70}\text{N}_4\text{O}_6$, 895.5374; found, 895.5385.

3c. Yield: 18%. mp 265–268 °C. FT-IR (KBr): $\nu = 1588, 1483, 1365, 1176, 1120, 938, 833, 784 \text{ cm}^{-1}$. $^1\text{H NMR}$ (300 MHz, CDCl_3 , TMS): δ 3.14–3.16 (m, 18H, $-\text{NCH}_3$), 3.54–3.65 (m, 16H, $-\text{NCH}_2$, and $-\text{OCH}_2$), 6.73–6.78 (dd, $J = 1.35, 9.3 \text{ Hz}$, 8H, aromatic), 8.3–8.36 (dd, $J = 2.25, 9.1 \text{ Hz}$, 8H, aromatic). $^{13}\text{C NMR}$: δ 39.66, 40.29, 52.38, 68.53, 70.52, 70.58, 70.63, 70.89, 112.35, 112.53, 119.86, 120.2, 133.17, 154.77, 154.98, 183.36. MALDI-TOF MS (MW = 770.922): $m/z = 771.09 [\text{M} + \text{H}]^+$. Anal. Calcd for $\text{C}_{46}\text{H}_{50}\text{N}_4\text{O}_7$: C, 71.67; H, 6.54; N, 7.27. Found: C, 71.36; H, 6.78; N, 7.06.

Preparation of the Monochromophore 4a. To a 100 mL round-bottomed flask containing 50 mL of 2-propanol were added **1a** (100 mg, 0.35 mmol), **2b** (105 mg, 0.35 mmol), and tributyl orthoformate (1 mL). After being refluxed for 12 h, the hot reaction mixture was filtered, and the solid was washed with 2-propanol until the filtrate was almost colorless. Column chromatography (chloroform/methanol, 95:5) of the crude product over silica gel (100–200 mesh) gave the pure product **4a**. Yield: 32%. mp 112–114 °C. FT-IR (KBr): $\nu = 1580, 1351, 1270, 1169, 1108, 784 \text{ cm}^{-1}$. $^1\text{H NMR}$ (300 MHz, CDCl_3 , TMS): δ 0.96–1.01 (t, $J = 7.26 \text{ Hz}$, 6H, $-\text{CH}_3$), 1.25–1.43 (m, 8H, $-\text{CH}_2$), 2.92 (s, 3H, $-\text{NCH}_3$), 3.13 (s, 3H, $-\text{NCH}_3$), 3.41–3.65 (m, 12H, $-\text{NCH}_2$, and $-\text{OCH}_2$), 6.7–6.77 (m, 7H, aromatic), 7.18–7.25 (t, $J = 7.9 \text{ Hz}$, 2H, aromatic), 8.36–8.39 (dd, $J = 2.35, 9.35 \text{ Hz}$, 4H, aromatic) ppm. $^{13}\text{C NMR}$ (75 MHz, CDCl_3): δ 13.8, 20.2, 29.6, 38.9, 39.5, 51.2, 52.3, 52.4, 68.7, 69.1, 112.1, 112.2, 112.3, 116.3, 119.4, 122.03, 129.1, 132.8, 133.5, 153.7, 183.4 ppm. MALDI-TOF MS (MW = 567.7): $m/z = 568.3 [\text{M} + \text{H}]^+$. Anal. Calcd for $\text{C}_{56}\text{H}_{70}\text{N}_4\text{O}_6$: C, 76.16; H, 7.99; N, 7.40. Found: C, 75.84; H, 8.19; N, 7.54.

Acknowledgment. This paper is dedicated to Prof. M. V. George on the occasion of his 75th birthday. We thank the Department of Science and Technology, Government of India for financial support (DST/SF/C6/99-2000). We are grateful to Prof. Jörg Daub, Institute of Organic Chemistry, University of Regensburg for the HRMS data and for fruitful discussions. E.A. and P.C. thank CSIR, Government of India for a research fellowship. This is Contribution No. 180 from RRLT-PPD.

Supporting Information Available: Synthetic details of **1a–c**, **2a**, and **2b**, changes in the absorption and emission properties of **3a** with $\text{Sr}(\text{ClO}_4)_2$, $\text{Ba}(\text{ClO}_4)_2$, LiClO_4 , NaClO_4 , and KClO_4 , **3b** with $\text{Mg}(\text{ClO}_4)_2$, $\text{Ca}(\text{ClO}_4)_2$, $\text{Sr}(\text{ClO}_4)_2$, and $\text{Ba}(\text{ClO}_4)_2$, and **3c** with $\text{Mg}(\text{ClO}_4)_2$, $\text{Ca}(\text{ClO}_4)_2$, $\text{Sr}(\text{ClO}_4)_2$, and $\text{Ba}(\text{ClO}_4)_2$, plots of variation of quantum yield with $[\text{M}^{n+}]$, Job plots of **3b** with Mg^{2+} and Ca^{2+} ions, and Benesi–Hildebrand plots of **3a** and **3b** with Mg^{2+} ions. This material is available free of charge via the Internet at <http://pubs.acs.org>.

JA0393776